Structural Eng./Earthquake Eng., JSCE, Vol.25, No.1, 16s-24s, 2008
(Copy of Dobokugakkai Ronbunsyuu A Vol.64 No.2, 288-296, 2008.4)

# EXTREMELY LOW CYCLE FATIGUE ASSESSMENT METHOD FOR UN-STIFFENED CANTILEVER STEEL COLUMNS

Kazuo TATEISHI[1], Tao CHEN[2] and Takeshi HANJI[3]

[1]Member of JSCE, Professor, EcoTopia Science Institute, Nagoya University
(Furo-cho, Chikusa-ku, Nagoya 464-8603, Japan)
E-mail: tateishi@esi.nagoya-u.ac.jp
[2]Student Member of JSCE, Dept. of Civil Eng., Nagoya University
(Furo-cho, Chikusa-ku, Nagoya 464-8603, Japan)
E-mail: h045107d@mbox.nagoya-u.ac.jp
[3]Member of JSCE, Researcher, EcoTopia Science Institute, Nagoya University
(Furo-cho, Chikusa-ku, Nagoya 464-8603, Japan)
E-mail: thanji@esi.nagoya-u.ac.jp

This paper presents the results of un-stiffened cantilever column subjected to incremental or constant amplitude cyclic loading. The objectives of this study are to investigate the extremely low cycle fatigue life of the column and verify the proposed strain based approach. During the test, fatigue cracks initiated from the weld toe at the corner and propagated along the weld toe. Finally, the column ruptured without a local buckling. The failure of low cycle fatigue induced by large cyclic deformation has been elucidated. In a further step, the crack initiation life was estimated based on the local strain by proposed simple approach. It is indicated that correlation between the test result and the estimated life was good enough.

***Key Words:*** *extremely low cycle fatigue, steel columns, crack initiation and propagation, local strain approach*

## 1. INTRODUCTION

Several steel piers suffered extremely low cycle fatigue (ELCF) damage in the Great Hanshin Earthquake (1995), which raises concerns about their performance in future earthquakes. However, this type of damage in civil engineering has not been fully understood. Only a limited number of researches on fatigue strength in ELCF region, corresponding to the fatigue life of less than tens of cycles, have been carried out and design guidelines have not been established.

Under seismic loading, steel piers undergo large strain fluctuations of typically one to tens of cycles. And fracture at the base end of steel piers is one of the failure modes[1)]. This type of failure was also observed in the former researches[2),3)]. Recently, several models for an assessment of the ELCF life have been proposed at the material level[4),5)].

For welded joints, fatigue cracks usually initiate from a weld toe. Krawinkler and Zohrei[6)] investigated the fracture at the weldment of I shaped cantilever beam and proposed a relationship between the fatigue endurance and the plastic strain expressed by Coffin- Manson equation. Sakano et al.[7),8),9)] conducted a series of low cycle fatigue tests on the steel beam-column joint and the pier base joint subjected to constant amplitude loading, and assessed the fatigue life by the strain near the weld toe. Ge et al.[10),11)] introduced Gurson's micro void damage model to investigate the ductile crack initiation in steel piers under incremental cyclic loading and carried out tests on steel piers. But they did not consider the effect of local geometry shape of the weld toe.

In this study, ELCF tests on un-stiffened cantilever steel column specimens with relatively small width thickness ratio[7),11)] were performed. Based on the test results, the validity of the ELCF assessment method developed in the former researches was examined.

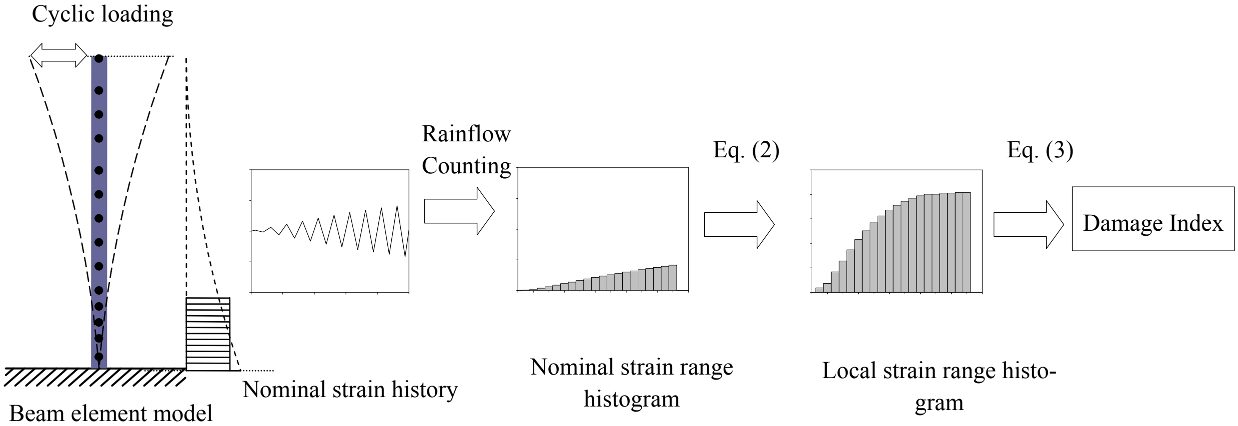


**Fig. 1** Extremely low cycle fatigue assessment for steel columns—conceptual overview

## 2. METHODOLOGY OF EXTREMELY LOW CYCLE FATIGUE ASSESSMENT

ELCF strength curves were obtained by a newly developed testing system[12] especially for a large strain field[5]. The results are expressed by Coffin -Manson equation,

$$\varepsilon_{ta} \cdot N^k = C \tag{1}$$

where $\varepsilon_{ta}$ is the total strain amplitude, $k$ and $C$ are the empirical constant listed in **Table 1**[5]. This criterion is developed based on the crack initiation life when the crack length attains 0.5mm.

Cracks usually initiate from the weld toe in welded joints. In this paper, the strain at the weld toe, i.e. cracking point, is called local strain. One possible way to assess the ELCF strength of welded joint can be proposed based on the local strain, so called local strain approach. Namely, after quantifying the local strain at the weld toe, the fatigue life can be predicted by referring the strength curves shown in Eq. (1). We have already applied this concept to T shaped weld joint and obtained a successful result[13]. In this trial, the local strain at the weld toe was obtained by finite element analysis with fine mesh.

It's not practicable, however, to use very fine mesh in engineering practice. Therefore, we tried to correlate the local strain range at the weld toe to the nominal strain range that can be obtained by averaging strain along effective failure length by beam element model. Here, the effective failure length is the smaller value of 0.7 times of the flange width and the diaphragm space, which was proposed in the previous research[14]. After extensive finite element analysis carried out on un-stiffened cantilever steel column, we finally established the correlation between the local strain range and the nominal strain range as follows[15],

**Table 1** Material parameters

| | $k$ | $C$ |
|---|---|---|
| Base metal | 0.587 | 0.392 |
| Deposited metal | 0.587 | 0.261 |
| Heat affected zone | 0.587 | 0.203 |

**Table 2** Parameters of strain range relationship

| Toe radius (mm) | $a$ | $b$ |
|---|---|---|
| 0.2 | -316.6 | 30.1 |
| 0.5 | -122.8 | 15.7 |
| 1.0 | -75.5 | 11.1 |
| 2.0 | -42.1 | 7.5 |

$\Delta\varepsilon_a/\varepsilon_y \le 35$ (where, $\varepsilon_y$ is the yield strain), the plate thickness ranges is from 12mm to 36mm, and the weld leg length ranges is from 6mm to 10mm.

$$\Delta\varepsilon_r / \Delta\varepsilon_a = a\Delta\varepsilon_a + b \tag{2}$$

where $\Delta\varepsilon_r$ is the local strain range, $\Delta\varepsilon_a$ is the nominal strain range. **Table 2** gives the parameters $a$ and $b$ with respect to the weld toe radius.

Based on these results, we proposed a simple fatigue assessment method in ELCF region. **Fig. 1** illustrates the conceptual overview of the ELCF assessment for un-stiffened cantilever steel column. The nominal strain history is obtained by beam analysis and processed to the nominal strain range histogram by rainflow counting method. The nominal strain range histogram can be converted to the local strain range histogram by Eq. (2).

To evaluate the cumulative damage, a linear cumulative damage rule is brought out by Miner[16].

$$D = \sum n_i / N_i \tag{3}$$

where $D$ is the damage index, $n_i$ and $N_i$ are the number of cycles under the constant amplitude loading and the fatigue life under the same loading, respectively. In engineering practice, fatigue failure is assumed to occur when $D$ attains 1.0.

To validate the proposed approach, experimental verifications are necessary. But available test results are limited, because geometry parameters of the weld toe were usually neglected in former researches. So

**Table 3** Geometry configuration and parameters of specimen

| Specimen | $h_1$ (mm) | $h_2$ (mm) | $I_1$ ($\times 10^7$mm$^4$) | $I_2$ ($\times 10^7$mm$^4$) | $R_f$ | $\bar{\lambda}$ | $\delta_y$ (mm) | $H_y$ (kN) |
|---|---|---|---|---|---|---|---|---|
| U1 | 550 | 133 | 1.5769 | 4.7289 | 0.2389 | 0.2979 | 4.12 | 159.05 |
| U2 | 775 | 208 | 1.5769 | 4.7289 | 0.2389 | 0.4197 | 7.96 | 112.87 |

**Table 4** Mechanical properties and chemical compositions

| SM490YA Flange and Web plate | Yield Stress (MPa) | Tensile Strength (MPa) | Elongation (%) | Chemical compositions (%) | | | | |
|---|---|---|---|---|---|---|---|---|
| | | | | C | Si | Mn | P | S |
| | 380 | 531 | 25 | 0.16 | 0.35 | 1.47 | 0.015 | 0.009 |

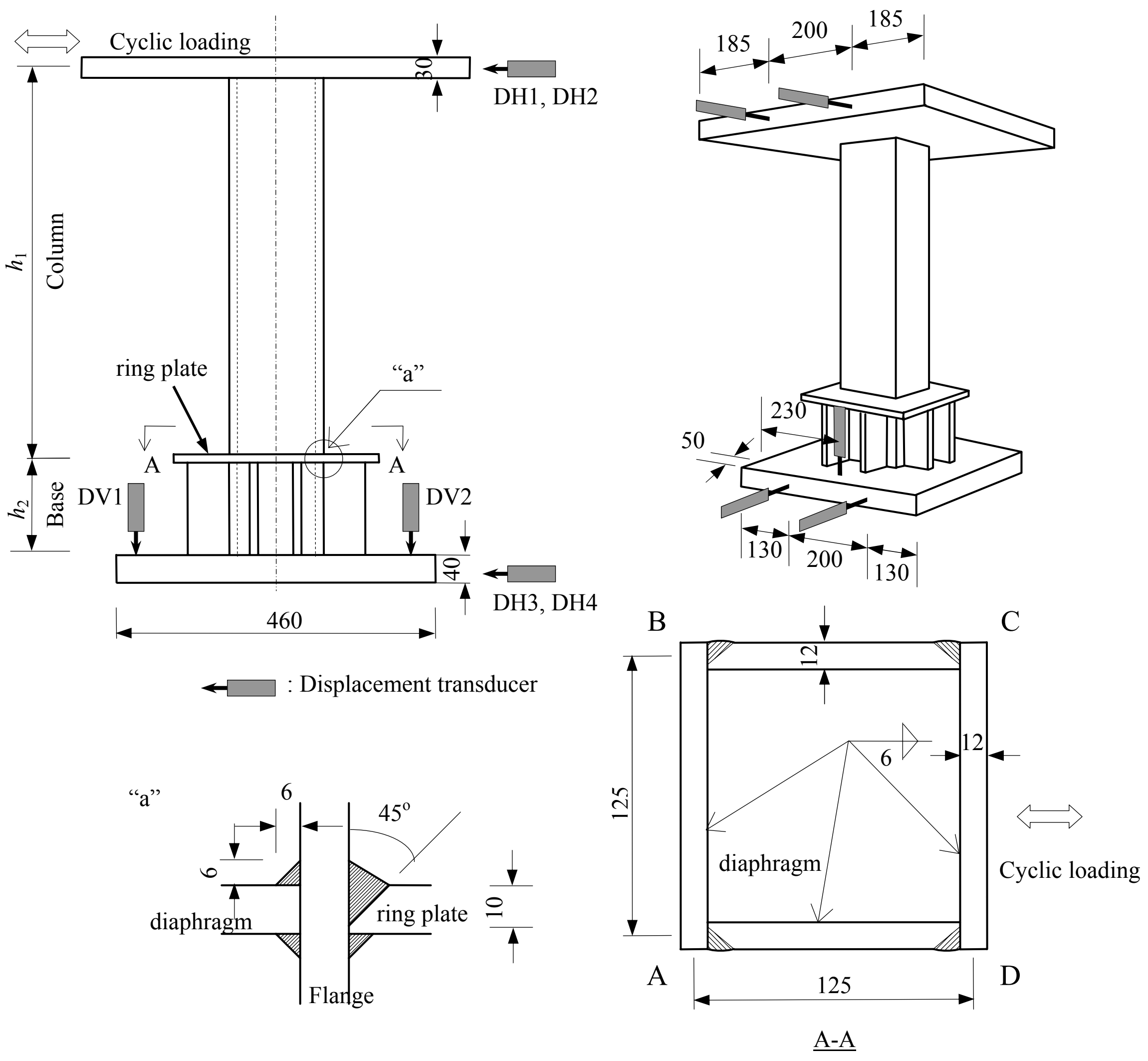


**Fig. 2** Configuration of test specimen

we carried out the ELCF test on un-stiffened cantilever steel column.

## 3. TEST PROGRAM

### (1) Specimen configuration

**Fig. 2** and **Table 3** show the configurations and dimensions of the specimens. They are un-stiffened cantilever steel columns with box section. Plate thickness is 12mm. Flange width and web breadth is 125mm. The width thickness ratio $R_f$ and the slenderness ratio $\bar{\lambda}$ are defined as follows,

$$R_f = \frac{b}{t}\sqrt{\frac{12(1-\nu^2)}{\pi^2\kappa}}\sqrt{\frac{\sigma_y}{E}} \tag{4}$$

$$\bar{\lambda} = \frac{Kh}{r}\frac{1}{\pi}\sqrt{\frac{\sigma_y}{E}} \tag{5}$$

where $b$ is the flange width, $t$ is the plate thickness, $\sigma_y$ is the yield stress, $E$ is Young's modulus, $\nu$ is Poisson's ratio, $\kappa$ is the buckling coefficient of a plate ($\kappa$=4.0), $h$ is the column height, $K$ is the effective length factor ($K$=2.0 for a fixed-free column), $r$ is the radius of gyration of the section.

In this study, in order to avoid the local bucking, relatively small width thickness ratio $R_f$, which was 0.2389, was taken[7),11)]. Two slenderness ratios $\bar{\lambda}$ were considered, which were 0.4179 and 0.2979.

Horizontal yield load $H_y$ and yield displacement $\delta_y$ in **Table 3** was calculated based on Timoshenko beam theory, which incorporates the shear deforma-

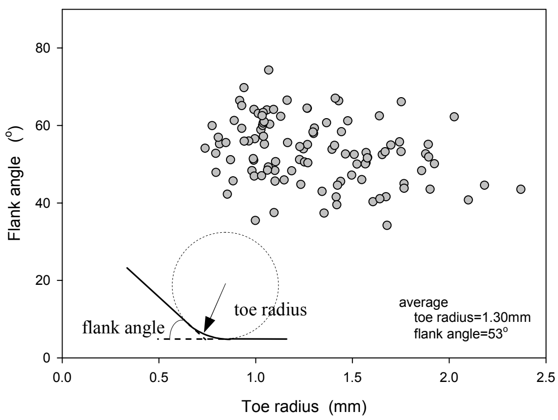


**Fig. 3** Measured toe radius and flank angle

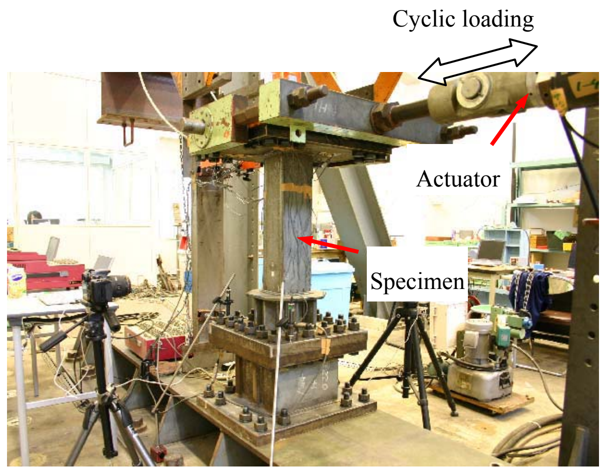


**Fig. 4** Test setup

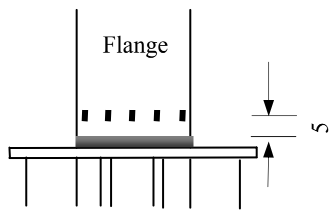


**Fig. 5** Arrangement of strain gauges

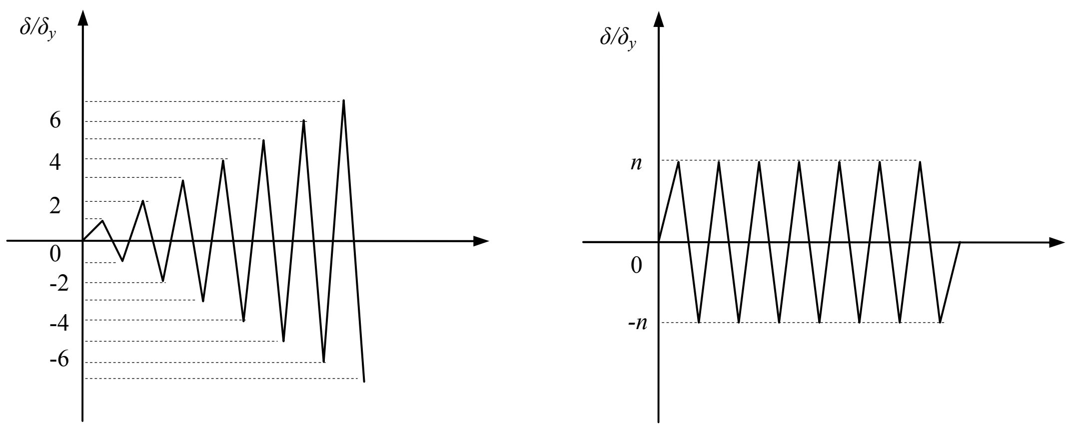


a) Incremental cyclic loading

b) Constant amplitude loading

**Fig. 6** Loading pattern

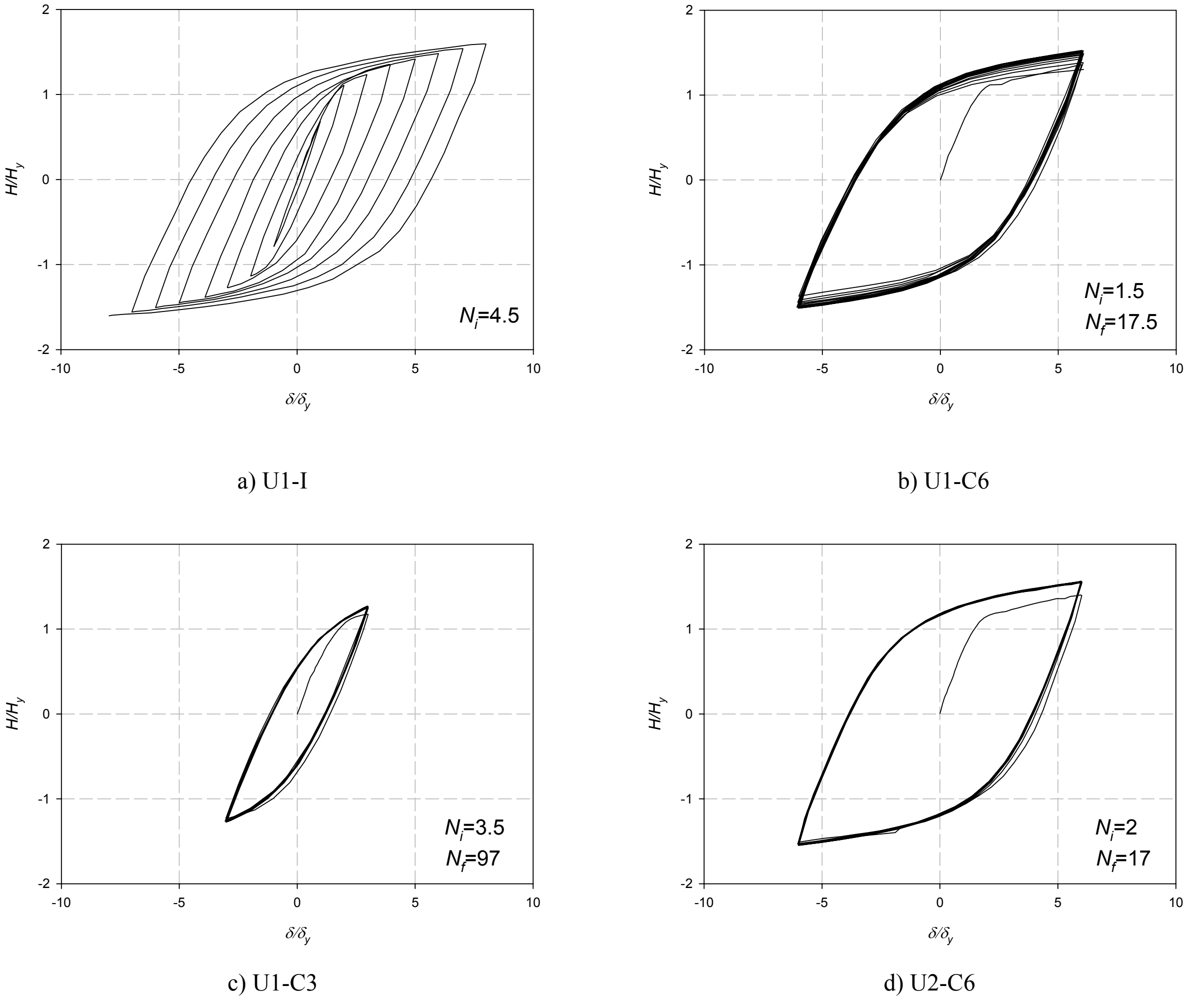


a) U1-I
b) U1-C6
c) U1-C3
d) U2-C6

**Fig. 7** Load-displacement hysteretic curves

tion. All specimens were made from SM490YA. The mechanical properties and chemical compositions are tabulated in **Table 4**. The welding method was $CO_2$ gas shielded semi-automatic welding with filler metal of 1.2 mm in diameter. The specimens were in as-welded state. Plate assembly of the base joint was similar to that commonly used in actual steel members.

The weld toe profile is essential to the local strain concentration. Basic geometry parameters of the weld bead, which are the weld toe radius and the flank angle, were measured by a silicon based impression material. The results are plotted in **Fig. 3**. They were measured near the corners where the cracks were observed during the test. For all results, the average toe radius was 1.30mm and the average flank angle was 53$^{o}$.

## (2) Test setup

**Fig. 4** illustrates test set up. Each specimen was bolted to the base and loaded at the top. Lateral quasi-static cyclic load was applied by an actuator. In

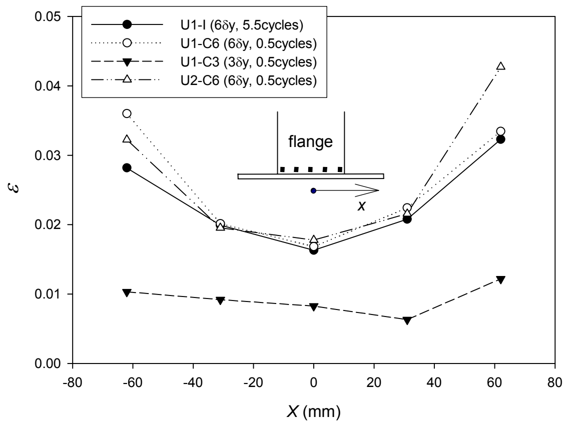


**Fig. 8** Strain distribution along flange

the current study, axial loading was not applied to the specimens because its effect on strain range is trivial[15]. Six displacement transducers were placed on the test column, as shown in **Fig. 2**. Four of them were used to acquire the horizontal displacement and two of them were placed vertically on the base plate to calculate the rotation. The top lateral displacement was calibrated by subtraction of base deformations.

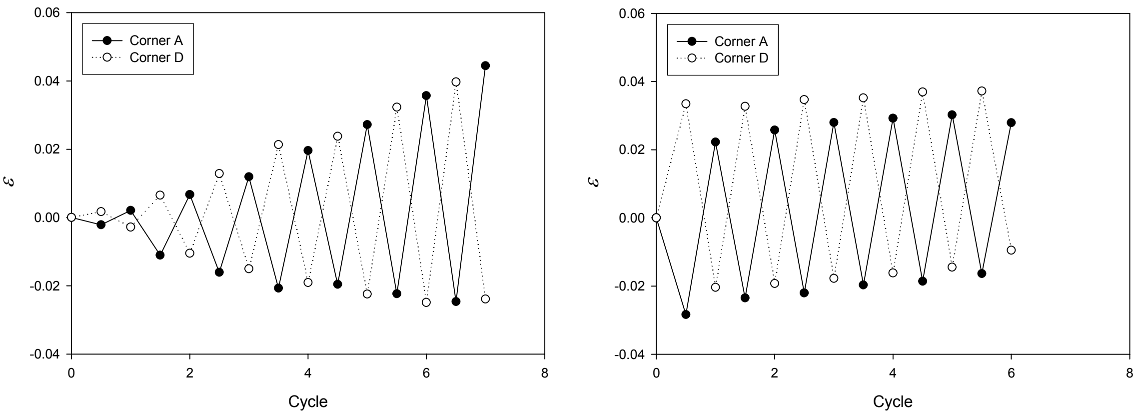


a) U1-I　　　b) U1-C6

**Fig. 9** Strain history near corner

a) Crack initiation at corner ($N$=4.5)　　b) Oblique crack at flange ($N$=18)　　c) Crack through flange ($N$=18.5)

**Fig. 10** Crack observation of pier (U1-C6)

The arrangement of strain gauges is shown in **Fig. 5**, which was installed along the flange and 5mm away from the weld toe on two sides. The gauge length was 2mm.

For convenience of identification during crack observation, corners are marked as A~D as shown in **Fig. 2**.

### (3) Loading pattern

The tests were conducted under displacement control for horizontal direction. Positive direction was defined as when corner C and D were initially under tension. Commonly used incremental cyclic loading procedure was employed for one specimen, as shown in **Fig. 6 a**), which was named U1-I. Constant amplitude loading, as shown in **Fig. 6 b**), was applied to other three specimens. The amplitude was 3 (U1-C3) or 6 (U1-C6 and U2-C6) times of yield displacement. Totally, four specimens were tested under different loading patterns.

## 4. TEST RESULTS AND OBSERVATIONS

### (1) Hysteretic curves

**Fig. 7** shows the load-displacement hysteretic curves of the specimens. The abscissa represents normalized horizontal displacement at the top $\delta/\delta_y$, whereas the ordinate indicates normalized load of the actuator $H/H_y$. Because of the limitation of testing devices, only initial several loops were measured and recorded.

The specimens were failed by stable crack growth instead of brittle fracture and no local buckling was observed through the test. In the figure, $N_i$ and $N_f$ denote the number of cycles to crack initiation and failure.

### (2) Strain distribution and history

**Fig. 8** shows typical strain distributions along flange (C-D side in **Fig. 2**), which were recorded by strain gauges 5mm away from the weld toe. Although these values cannot be directly used to assess the crack initiation life, they illustrate the general behavior of strains. It can be seen that strains near the corners were larger than those of inner parts. This is consistent with the numerical analysis results[15),17)]. The distribution was similar regardless of loading types and configurations of the specimens.

**Fig. 9** illustrates typical strain histories recorded by strain gauges at the corners on both flanges, which were results of incremental cyclic loading to speci-

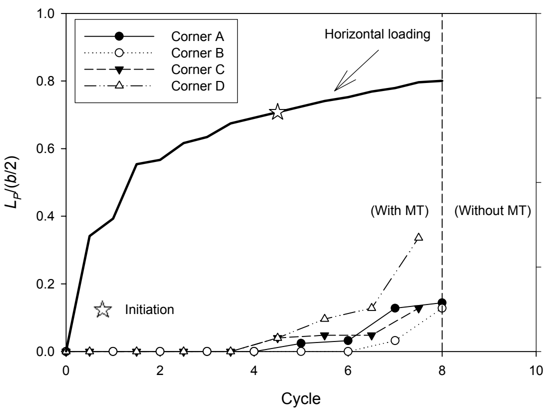


a) Crack propagation of U1-I

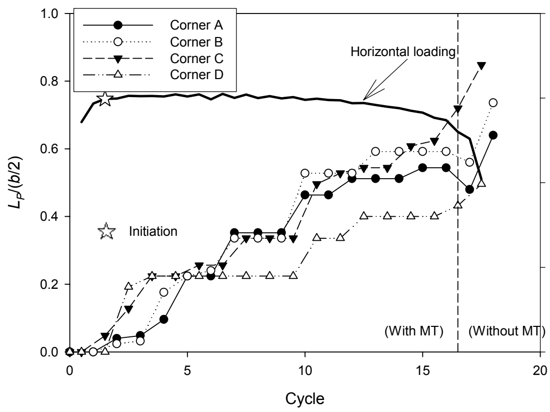


b) Crack propagation of U1-C6

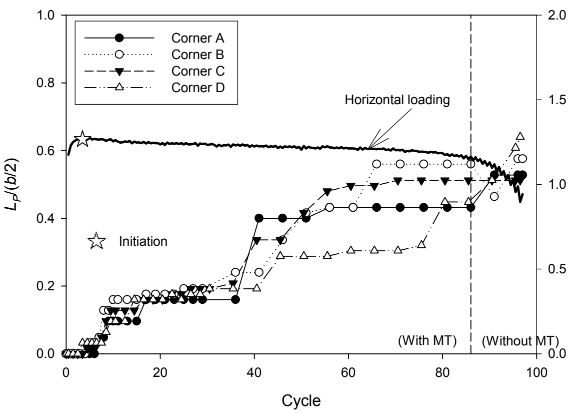


c) Crack propagation of U1-C3

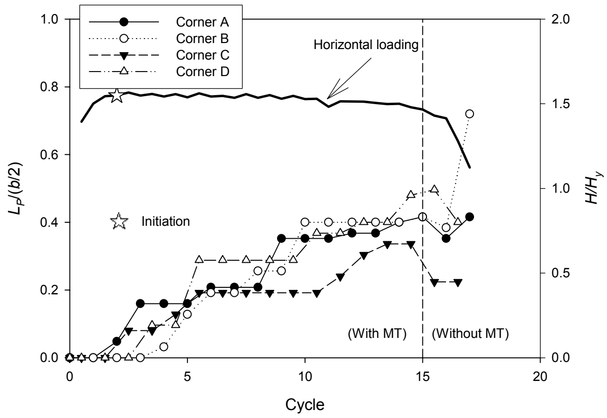


d) Crack propagation of U2-C6

**Fig. 11** Crack length of flange near corner

men U1-I and constant amplitude loading to specimen U1-C6 respectively. The strain attained as large as 4% that is far beyond the yield strain. Although the value of the strains was shifting gradually, the strain range was kept almost constant during the test.

**(3) Visual observations**

Crack observation was performed with Magnetic particle testing method (MT) at each half cycle.

During all of the tests, cracks initiated at corners of the specimens where strain concentration was large. For specimen U1-I, cracks were found at corner C and D at same time. And each crack length was approximately 2.5mm. For U1-C6, a 3.0mm length crack was firstly identified at corner C. For U1-C3, the crack initiation corner was D and its length was 2.0mm. For specimen U2-C6, the crack was observed with 3.0mm length at corner A. Taking specimen U1-C6 as an example, **Fig. 10 a)** provides a typical crack initiation at the corner, which was denoted by an arrow. It is also noted that the crack initiated from weld deposit at the weld toe. The initial cracks occurred at corners and propagated along the weld toe. With the propagation of crack length, oblique cracks formed in the flange and web plate before major strength degradation took place, as shown in **Fig. 10 b)**. **Fig. 10 c)** illustrates the final failure mode when the crack formed through the flanges.

**Fig. 11** summarizes all crack lengths of flanges around the corners. Meanwhile, horizontal loading is also plotted with cycles. Horizontal axis is the number of cycles, whereas left vertical axis indicates the crack length $L_P$ normalized by the half width of the flange $b/2$, and right vertical axis represents the horizontal loading $H$ normalized by the yield loading $H_y$. At the beginning of the test, MT observation was executed. Whereas crack length was measured without MT after the crack grew to a certain length. They are distinguished by a vertical dash line in the figure. Fatigue crack initiation points are also marked in the figure.

During the test, it was found that crack growth did not cause evident deterioration of the loading capacity and stiffness until the crack has grown up to approximately 0.6 times of the half flange width. Once deterioration took place, it occurred at a very high rate leading to failure.

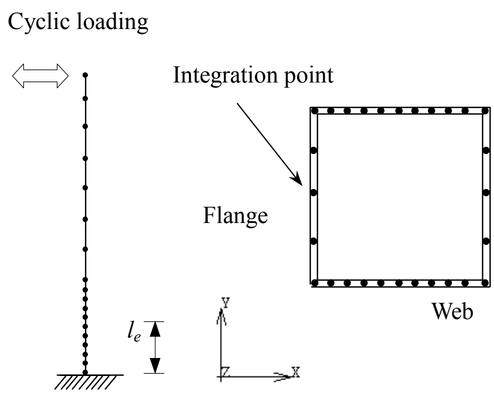


**Fig. 12** Illustrations of FE model

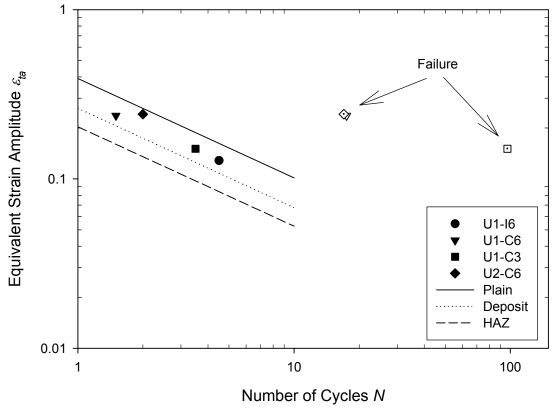


**Fig. 13** Local strain amplitude versus cycles to crack initiation

## 5. EXTREMELY LOW CYCLE FATIGUE ASSESSMENT OF STEEL COLUMNS

### (1) Analytical model

To apply the proposed approach presented in section 2, the beam element model of un-stiffened cantilever steel column was created, as shown in **Fig. 12**. It was realized by two-node 3D type beam element incorporated in MSC.Marc. For box section, 28 integration points were specified, which was determined after considering the software's capacity and referring to other's researches[18]. In the figure, $l_e$ denotes the effective failure length of the column. Here, five elements are assigned along $l_e$. It was determined after comparing the average strain in $l_e$ with 5, 10, 15 and 20 partitions along $l_e$.

A bilinear constitutive material model, which had the yield stress of 380MPa and Young's modulus of $2\times10^5$MPa, was adopted. Poisson's ratio was 0.3 and strain-hardening ratio, which is the ratio between the post-yield tangent and the initial elastic tangent, was assumed as 1/100. The kinematic hardening was used with von Mises yield criterion.

### (2) Analytical results

After numerical analysis, the history of the nominal strain, which is the average strain at integration points in the flange along effective failure length, was acquired and processed into strain range histograms by rainflow counting method. They were converted to local strain range histograms by Eq. (2) according to the weld toe radius. In this study, the weld toe radius was obtained by statistical analyses with measured results shown in **Fig. 3**. Lower bound of a 95% confidence interval was taken. So the weld toe radius was 0.60mm. Flank angle was set as 45$^o$ since its influence on the local strain distribution is negligible[13]. Then parameters $a$ and $b$ in Eq. (2) were obtained by interpolation from **Table 2**.

Then the number of cycles to crack initiation versus the equivalent strain amplitude is plotted in **Fig. 13**. ELCF strength curves obtained in the former researches[5] are also graphed. Solid line represents the fatigue strength of plain material. Dotted line and dashed line are reflections of weld deposit and HAZ respectively. Data points should be compared with the strength curve for the weld deposit, because crack initiation locations were in the weld deposit at the weld toe. All data are slightly above the fatigue strength curve for the weld deposit. This maybe partly owe to inconsistency between the crack initiation lengths, which were 2.0~3.0mm in the tests, while the strength curves were based on the 0.5mm crack initiation length. Except this discrepancy, the proposed approach can predict the crack initiation life in ELCF region with enough accuracy regardless of loading patterns and specimen geometries.

Failure lives, which are the number of cycles when the loading capacity decreased to 80% of the maximum value, were also plotted. They were longer than the initiation life. In this study, the specimens were failed by the stable crack growth instead of the brittle fracture. As a result, the failure life was longer than the crack initiation life. We need to take further investigations on the relationship between the crack initiation life and the crack propagation life.

## 6. SUMMARY AND CONCLUSIONS

This paper describes an experimental investigation on extremely low cycle fatigue of un-stiffened cantilever steel column with box section. In particular, this experimental study focused on the crack initiation at weld toe. Test results are used to validate the strain based approach proposed in former research.

The following main conclusions can be stated as follows:

1) Extremely low cycle fatigue cracks initiated from the weld toe at corners of the specimen.
2) The loading capacity of the specimen did not deteriorate until the crack grew up to significant length.
3) Proposed simple strain based approach can be used to predict the number of cycles to the extremely low cycle fatigue crack initiation.

**ACKNOWLEDGMENT:** This research was funded by Ministry of Education, Culture, Sports, Science and Technology under grand number B (2) 18360217. The advices of Prof. Hanbin Ge (Nagoya University) and Prof. Akira Kasai (Nagoya University) are greatly appreciated. We would also like to thank Dr. Hirotaka Oda (The Takigami Steel Construction Co., Ltd.) for his assistance during manufacture of specimens.

## REFERENCES

1) Okashita, K., Ohminami, R., Michiba, K., Yamamoto, A., Tomimatsu, M., Tanji, Y. and Miki, C.: Investigation of the brittle fracture at the corner of P75 rigid-frame pier in Kobe Harbor Highway during the Hyogoken-nanbu Earthquake, *Journal of Structural Mechanics and Earthquake Engineering*, JSCE, Vol. I-43, No.591, pp.243-261, 1998. (in Japanese)
2) Tominaga, T., and Yasunami, H.: An experimental study on ductility of steel bridge piers with thick walled cross section and small number of stiffeners, *Journal of Structural Engineering*, JSCE, Vol. 40A, pp.189-200, 1994. (in Japanese)
3) Ge, H.B. and Usami, T.: Cyclic tests of concrete-filled steel box columns, *Journal of Structural Engineering*, ASCE, Vol. 122, No.10, pp.1169-1177, 1996.
4) Masatoshi, K.: Extremely low cycle fatigue life prediction based on a new cumulative fatigue damage model, *International Journal of Fatigue*, Vol. 24, pp.699-703, 2001.
5) Tateishi, K., Hanji, T. and Minami, K.: A prediction model for extremely low cycle fatigue strength of structural steel, *International Journal of Fatigue*, Vol. 29, pp.887-896, 2007.
6) Krawinkler, H. and Zohrei, M.: Cumulative damage in steel structures subjected to earthquake ground motions, *Computers & Structures*, Vol. 16, No. 1-4, pp.531-541, 1983.
7) Sakano, M., Mikami, I., Murayama, H. and Misumi, Y.: Super-Low-Cycle fatigue behavior of steel pier base joint, *Steel Construction Engineering*, Vol. 2, No.8, pp.73-82, 1995. (in Japanese)
8) Sakano, M. and Wahab, M.A.: Extremely low cycle (ELC) fatigue cracking behaviour in steel bridge rigid frame piers, *Journal of Materials Processing Technology*, Vol. 118, pp.36-39, 2001.
9) Sakano, M., Mikami, I. and Takaba, S.: Low cycle fatigue behavior of steel pier beam-column joint, *Journal of Structural Mechanics and Earthquake Engineering*, JSCE, Vol. I-39, No. 563, pp.49-60, 1997. (in Japanese)
10) Ge, H.B., Kawahito, M. and Ohashi, M.: Fundamental study on ductile crack initiation condition in structural steels considering mirco-void growth, *Journal of Earthquake Engineering*, JSCE, No.28, Paper No.190, 2005. (in Japanese)
11) Ge, H.B., Ohashi, M. and Tajima, R.: Experimental study on ductile crack initiation and its propagation in steel bridge piers of thick-walled box section, *Journal of Structural Engineering*, JSCE, Vol. 53A, pp.493-502, 2007. (in Japanese)
12) Tateishi, K. and Hanji, T.: Low cycle fatigue strength of butt welded steel joint by means of new testing system with image technique, *International Journal of Fatigue*, Vol. 26, No.12, pp.1349-1356, 2004.
13) Hanji, T., Tateishi, K., Minami, K. and Kitoh, K.: Extremely low cycle fatigue assessment for welded joints based on peak strain approach, *Journal of Structural Mechanics and Earthquake Engineering*, JSCE, Vol. I-74, No.808, pp.137-145, 2006. (in Japanese)
14) Zheng, Y., Usami, T., and Ge, H. B.: Ductility evaluation procedure for thin-walled steel structures, *Journal of Structural Engineering*, ASCE, Vol. 126, No.11, pp.1312–1319, 2000.
15) Chen, T. and Tateishi, T.: Extremely low cycle fatigue assessment of thick walled steel pier using local strain approach, *Journal of Structural Engineering*, JSCE, Vol. 53A, pp.485-492, 2007.
16) Miner, M. A.: Cumulative damage in fatigue, Transactions, *American Society of Mechanical Engineers*, Vol. 67, pp. A159-A164, 1945.
17) Matsui, N. and Ge, H.B.: Evaluation of Strain Concentration for Prediction of Ductile Crack Initiation in Steel Bridge Piers, *Proceedings of the Eighth International Summer Symposium*, Nagoya, Japan, pp.31-34, July 29, 2006.
18) For example, Usami, T., Lu, Z., Ge, H.B. and Kono, T.: Seismic performance evaluation of steel arch bridges against major earthquakes. Part 1: Dynamic analysis approach, *Earthquake Engineering and Structural Dynamics*, Vol. 33, pp.1337-1354, 2004.

**(Received June 19, 2007)**